Available online at www.sciencedirect.com
SCIENCE DIRECT®
Journal of Sound and Vibration 291 (2006) 81–99
JOURNAL OF SOUND AND VIBRATION
www.elsevier.com/locate/jsvi

Analysis of the energy transmission in compound cylindrical shells with and without internal heavy fluid loading by boundary integral equations and by Floquet theory

S.V. Sorokin[a,*], O.A. Ershova[b]

[a]Institute of Mechanical Engineering, Aalborg University, Pontoppidanstraede 101, DK 9220 Aalborg, Denmark
[b]Department of Engineering Mechanics, State Marine Technical University of St. Petersburg, St. Petersburg, 190008, Russian Federation

Received 19 March 2004; received in revised form 23 May 2005; accepted 31 May 2005
Available online 21 October 2005

Abstract

This paper addresses three aspects of the steady-state free vibration of non-uniform (i.e., composed of alternating elements) elastic cylindrical shells with and without internal heavy fluid loading, which have not previously been studied in detailed form. Firstly, Floquet theory is applied to detect the location of frequency band gaps in an infinitely long periodic fluid-filled cylindrical shell vibrating in the 'beam-type' mode $m = 1$ and in the ovalling mode $m = 2$ in the framework of two simplified theories. As a prerequisite for this study, the validity range of these theories is estimated by comparison of the resulting dispersion curves with the exact solution. Secondly, the boundary equations are derived for a cylindrical shell with internal heavy fluid loading in the framework of the suggested theories. The methodology of boundary integral equations is used to obtain exact solutions for the problems of free vibrations of a finite shell and wave propagation in an infinitely long shell. Finally, the energy transmission in a semi-infinite non-uniform cylindrical shell with and without internal heavy fluid loading is addressed; predictions obtained by use of Floquet theory are compared with the exact solution obtained by the method of boundary integral equations.

1. Introduction

Analysis of vibroacoustic energy transmission in pipelines is an important and challenging problem in various industrial and civil applications. The ability to carry out 'quiet design' of, for example, heating systems in houses as well as the noise and vibration control of oil- and gas-transporting industrial pipelines is necessary to meet modern regulations. In these systems, the source of energy is a pump or a valve and the sound and vibration is identified as a by-product of their intended effect. The excitation of vibration in a fluid-conveying pipeline typically occurs in a relatively low-frequency band and the total energy input is distributed between several circumferential modes in a fluid-filled pipe, considered as a cylindrical shell under internal heavy fluid loading. From the viewpoint of noise and vibration control, it is expedient to trace the energy input back to the mechanical and acoustical sources associated with the operation of the pump or valve. Experimental

*Corresponding author.
E-mail address: svs@ime.aau.dk (S.V. Sorokin).

0022-460X/$ - see front matter © 2005 Elsevier Ltd. All rights reserved.
doi:10.1016/j.jsv.2005.05.031

results and theoretical analysis both suggest that highest importance should be attributed to modes with low circumferential wavenumbers, in particular the 'breathing mode' $m = 0$ and the 'beam mode' $m = 1$ (see Ref. [1]). The former is excited predominantly by acoustical sources, whereas the latter as well as all higher-order modes are mainly excited mechanically. The 'breathing' and the 'beam' modes are able to transport vibroacoustic energy along the pipe at any excitation frequency, whereas all the other modes have so-called 'cut-off' frequencies and are able to participate in energy transmission over long distances only when the excitation frequency exceeds its 'cut-off' value.

Suppression of the energy transmission in a cylindrical shell filled with a fluid may be achieved by various types of structural and acoustic 'anechoic termination' (see, for example, Refs. [1,2]), and it is not the goal of this paper to survey these. Rather, the attention here is focused on one particular tool—the use of alternating elements to generate the effect of a frequency band gap in a periodic structure. In an earlier paper [3], Floquet theory [4,5] has been used to study the location of frequency band gaps in an infinitely long non-uniform cylindrical shell with and without internal heavy fluid loading, which vibrates in the 'breathing mode' $m = 0$, and it has been shown that suppression of wave propagation is feasible within relatively narrow 'band gaps'. Here, the same methodology is extended to capture the 'band gap' phenomenon for an arbitrary circumferential wavenumber in a cylindrical shell, and examples for the cases $m = 1$ and 2 are given.

The present paper also has several other objectives, concerned with placing the immediate application of Floquet theory (for the analysis of wave propagation in an unbounded periodic cylindrical shell) into somewhat broader theoretical and practical context. Firstly, two simplified theories of wave propagation in a shell with heavy internal fluid loading are proposed and their validity ranges are estimated. Secondly, the methodology of boundary integral equations is used to obtain the exact solution of a problem of wave propagation in a fluid-filled semi-infinite shell, when the shell is composed of a small number of alternating elements. Finally, the predictions obtained from Floquet theory are validated by computations of the input mobility of a shell inside and outside the frequency band gaps.

This paper is structured as follows: in Section 2, the 'generic' problem of wave propagation in a uniform cylindrical shell with heavy internal fluid loading is considered and the ranges of validity of two simplified theories are estimated. In Section 3, these two theories are applied in the framework of Floquet methodology to detect the location and the width of frequency band gaps in a periodic cylindrical shell composed of an infinitely large number of alternating elements. The boundary equations for a cylindrical shell under heavy internal fluid loading are presented in Section 4. The eigenfrequencies of an empty cylindrical shell of the finite length are compared with those of a fluid-filled one for several typical combinations of boundary conditions. The formulation of a problem of wave propagation in a semi-infinite non-uniform cylindrical shell with and without heavy internal fluid loading in the framework of boundary equations method is presented in Section 5. The exact solution of this problem, obtained in a case, when a shell is composed of small number of alternating elements is compared with the predictions from Floquet theory in Section 6. The results obtained in the paper are summarized in Section 7.

2. Dispersion equations for a cylindrical shell under heavy loading

Steady-state wave propagation is considered in the framework of Goldenveizer–Novozhilov theory of thin shells [6] and conventional linear acoustics. A time dependence of all functions is chosen as $\exp(-\mathrm{i}\omega t)$, the circumferential modal decomposition is performed and wave motions at each individual wavenumber m are considered independently upon all others. The multiplier $\exp(\mathrm{i}m\theta - \mathrm{i}\omega t)$ is omitted from all the expressions that follow, and subscript m is used to denote a circumferential Fourier component.

2.1. General theory of thin shells

The governing equations, which describe propagation of free waves in a cylindrical shell filled with a compressible fluid, are

$$-\frac{\mathrm{d}^2 u_m}{\mathrm{d}x^2} + \frac{1-\nu}{2}\frac{m^2}{R^2}u_m - \frac{1+\nu}{2}\frac{m}{R}\frac{\mathrm{d}v_m}{\mathrm{d}x} - \frac{\nu}{R}\frac{\mathrm{d}w_m}{\mathrm{d}x} - \frac{\rho\omega^2(1-\nu^2)}{E}u_m = 0, \tag{1a}$$

$$\frac{1+\nu}{2}\frac{m}{R}\frac{\mathrm{d}u_m}{\mathrm{d}x}-\frac{1-\nu}{2}\frac{\mathrm{d}^2v_m}{\mathrm{d}x^2}+\frac{m^2}{R^2}v_m-\frac{h^2}{12}\frac{2(1-\nu)}{R^2}\frac{\mathrm{d}^2v_m}{\mathrm{d}x^2}+\frac{h^2}{12}\frac{m^2}{R^4}v_m+\frac{m}{R^2}w_m+\frac{h^2}{12}\frac{m^3}{R^4}w_m-\frac{h^2}{12}\frac{(2-\nu)m}{R^2}\frac{\mathrm{d}^2w_m}{\mathrm{d}x^2}-\frac{\rho\omega^2(1-\nu^2)}{E}v_m=0, \tag{1b}$$

$$\frac{\nu}{R}\frac{\mathrm{d}u_m}{\mathrm{d}x}+\frac{m}{R^2}v_m+\frac{h^2}{12}\frac{m^3}{R^4}v_m-\frac{h^2}{12}\frac{(2-\nu)m}{R^2}\frac{\mathrm{d}^2v_m}{\mathrm{d}x^2}+\frac{1}{R^2}w_m+\frac{h^2}{12}\frac{\mathrm{d}^4w_m}{\mathrm{d}x^4}-\frac{h^2}{12}\frac{2m^2}{R^2}\frac{\mathrm{d}^2w_m}{\mathrm{d}x^2}+\frac{h^2}{12}\frac{m^4}{R^4}w_m-\frac{\rho\omega^2(1-\nu^2)}{E}w_m-\frac{\mathrm{i}\omega\rho_{fl}(1-\nu^2)R}{Eh}\varphi_m=0, \tag{1c}$$

$$\frac{\partial^2\varphi_m}{\partial r^2}+\frac{1}{r}\frac{\partial\varphi_m}{\partial r}-\frac{m^2}{r^2}\varphi_m+\frac{\partial^2\varphi_m}{\partial x^2}+\frac{\omega^2}{c_{\mathrm{fl}}^2}\varphi_m=0, \tag{1d}$$

$$\left.\frac{\partial\varphi_m}{\partial r}\right|_{r=R}=-\mathrm{i}\omega w_m. \tag{1e}$$

In these equations (u_m, v_m, w_m) are components of the vector of displacements of a shell in the axial, circumferential and radial directions, respectively (see Fig. 1a), and φ_m is a velocity potential. The positive direction of a radial displacement coincides with the positive direction of a radial coordinate. Material properties of a shell, which has a thickness h and a radius R, are specified by the density ρ, Young's modulus E and Poisson ratio ν. The density of a fluid is introduced as ρ_{fl} and the sound speed is c_{fl}.

The force and moment resultants in a cross-section of the shell (see Fig. 1b), which are involved in the boundary and continuity conditions, are defined as (see also Ref. [7]):

$$Q_{1m}=\frac{Eh}{1-\nu^2}\left(\frac{\mathrm{d}u_m}{\mathrm{d}x}+\frac{m\nu}{R}v_m+\frac{\nu}{R}w_m\right), \tag{2a}$$

$$Q_{2m}=\frac{Eh}{1-\nu^2}\left(-\frac{1-\nu}{2}\frac{m}{R}u_m+\frac{1-\nu}{2}\frac{\mathrm{d}v_m}{\mathrm{d}x}+\frac{h^2}{12}\frac{2(1-\nu)}{R^2}\frac{\mathrm{d}v_m}{\mathrm{d}x}+\frac{h^2}{12}\frac{2(1-\nu)m}{R^2}\frac{\mathrm{d}w_m}{\mathrm{d}x}\right), \tag{2b}$$

$$Q_{3m}=-\frac{Eh^3}{12(1-\nu^2)}\left[\frac{\mathrm{d}^3w_m}{\mathrm{d}x^3}-\frac{(2-\nu)m^2}{R^2}\frac{\mathrm{d}w_m}{\mathrm{d}x}-\frac{(2-\nu)m}{R^2}\frac{\mathrm{d}v_m}{\mathrm{d}x}\right], \tag{2c}$$

$$Q_{4m}=\frac{Eh^3}{12(1-\nu^2)}\left[\frac{\mathrm{d}^2w_m}{\mathrm{d}x^2}-\frac{m^2\nu}{R^2}w_m-\frac{m\nu}{R^2}v_m\right]. \tag{2d}$$

These formulas present the axial 'membrane' force, the circumferential 'membrane' force, the radial shear force and the axial bending moment, respectively.

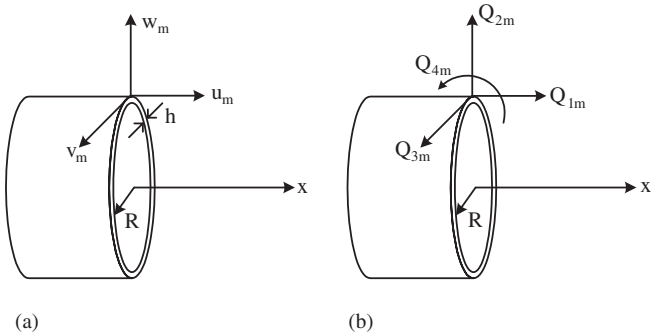

Fig. 1. A cylindrical shell: (a) modal displacements and (b) generalized modal forces.

2.2. Simplified theory of beam-type motions, $m = 1$

Probably the most 'natural' type of motion of a long tube is its vibration in the 'beam-type' mode, i.e., when the number of circumferential waves is $m = 1$. Although the general theory (1a)–(1e) is perfectly valid in this case, a considerable simplification of these equations may be introduced to speed up computations needed to obtain characteristics of wave propagation. Specifically, no distortion of the cross-sectional shape occurs in this case and the following links between displacements are established:

$$v_1(x) = -w_1(x), \tag{3a}$$

$$u_1(x) = -R\frac{\mathrm{d}w_1(x)}{\mathrm{d}x}. \tag{3b}$$

Then the following differential equation of beam-like motion of a shell with fluid loading is obtained

$$\frac{Eh}{1-\nu^2}\left(R^2+\frac{h^2}{12}\right)w_1'''' + \rho_0 hR^2\omega^2 w_1'' - 2\rho_0 hR^2\omega^2 w_1 + \mathrm{i}\rho_{\mathrm{fl}}\omega\varphi_1 = 0. \tag{4}$$

The velocity potential φ_1 is governed by the differential equation (1d) and the boundary condition (1e).

The generalized displacements are w_1, w_1' and the generalized forces (components Q_{11}, Q_{21} are absent likewise their counterparts u_1, v_1) are formulated as

$$Q_{31} = -\frac{Eh}{1-\nu^2}\left(R^2+\frac{h^2}{12}\right)\frac{\mathrm{d}^3 w_1}{\mathrm{d}x^3}, \tag{5a}$$

$$Q_{41} = \frac{Eh}{1-\nu^2}\left(R^2+\frac{h^2}{12}\right)\frac{\mathrm{d}^2 w_1}{\mathrm{d}x^2}. \tag{5b}$$

It is remarkable to note that this simple 'beam' theory is equally applicable to study wave motion in a shell filled in by a compressible and by an incompressible fluid since the assumptions (3a) and (3b) do not concern the behaviour of the fluid inside a tube.

A solution to the set of homogeneous differential equations (1) is sought as (k_{dim} is a dimensional wavenumber and propagating waves correspond to its purely imaginary values)

$$\begin{aligned} u_m(x) &= A_m \exp(k_{\mathrm{dim}}x),\\ v_m(x) &= B_m \exp(k_{\mathrm{dim}}x),\\ w_m(x) &= C_m \exp(k_{\mathrm{dim}}x),\\ \varphi_m(x,r) &= \hat{\varphi}_m(r)\exp(k_{\mathrm{dim}}x). \end{aligned} \tag{6}$$

The function $\hat{\varphi}_m(r)$ is determined from the following reduced problem

$$\frac{\mathrm{d}^2\hat{\varphi}_m}{\mathrm{d}r^2} + \frac{1}{r}\frac{\mathrm{d}\hat{\varphi}_m}{\mathrm{d}r} - \frac{m^2}{r^2}\hat{\varphi}_m + \left(k_{\mathrm{dim}}^2 + \frac{\omega^2}{c_{\mathrm{fl}}^2}\right)\hat{\varphi}_m = 0, \tag{7a}$$

$$\left.\frac{\mathrm{d}\hat{\varphi}_m}{\mathrm{d}r}\right|_{r=R} = -\mathrm{i}\omega C_m. \tag{7b}$$

Its solution is

$$\hat{\varphi}_m(r) = -\mathrm{i}\omega C_m J_m\left(r\sqrt{k_{\mathrm{dim}}^2+\frac{\omega^2}{c_{\mathrm{fl}}^2}}\right)\left[\left.\frac{\mathrm{d}J_m\left(r\sqrt{k_{\mathrm{dim}}^2+\frac{\omega^2}{c_{\mathrm{fl}}^2}}\right)}{\mathrm{d}r}\right|_{r=R}\right]^{-1}\exp(k_{\mathrm{dim}}x). \tag{8}$$

The sound speed in the shell material is introduced as $c^2 \equiv E/(\rho(1-\nu^2))$ and the scaled co-ordinates are $\tilde{r} = r/R$, $\tilde{x} = x/R$. The following non-dimensional parameters are used hereafter:

$$\Omega^2 = \frac{\rho(1-\nu^2)\omega^2 R^2}{E}, \quad \tilde{\rho} = \frac{\rho}{\rho_{\mathrm{fl}}}, \quad \tilde{\gamma} = \frac{c}{c_{\mathrm{fl}}}, \quad k = k_{\mathrm{dim}} R, \quad \kappa^2 = k^2 + \tilde{\gamma}^2 \Omega^2.$$

Then dispersion equation for a shell filled with a compressible fluid is formulated as

$$\begin{vmatrix} d_{11} & d_{12} & d_{13} \\ d_{21} & d_{22} & d_{23} \\ d_{31} & d_{32} & d_{33} \end{vmatrix} = 0 \tag{9}$$

with the following elements:

$$d_{11} = -k^2 + \frac{1-\nu}{2} m^2 - \Omega^2,$$

$$d_{12} = -\frac{1+\nu}{2} km = -d_{21},$$

$$d_{13} = -\nu k = -d_{31},$$

$$d_{22} = -\frac{1-\nu}{2} k^2 + m^2 - \Omega^2 - \frac{h^2}{12R^2} 2(1-\nu)k^2 + \frac{h^2}{12R^2} m^2,$$

$$d_{23} = m + \frac{h^2}{12R^2} m^3 - \frac{h^2}{12R^2} (2-\nu) m k^2 = d_{32},$$

$$d_{33} = 1 + \frac{h^2}{12R^2} k^4 - \frac{h^2}{12R^2} 2m^2 k^2 + \frac{h^2}{12R^2} m^4 - \Omega^2 - \tilde{\rho}\Omega^2 \frac{R}{h} J_m(\kappa) \left(\frac{\mathrm{d}J_m(\kappa\tilde{r})}{\mathrm{d}\tilde{r}} \bigg|_{\tilde{r}=1} \right)^{-1}.$$

To identify the type of a wave characterized by a root k_{mj} of this dispersion equation, the modal coefficients are introduced as

$$\alpha_{mj} = \frac{A_{mj}}{C_{mj}}, \quad \beta_{mj} = \frac{B_{mj}}{C_{mj}}. \tag{10}$$

They are found by solving the following system of equations:

$$\begin{aligned} d_{11}\alpha_{mj} + d_{12}\beta_{mj} &= -d_{13}, \\ d_{21}\alpha_{mj} + d_{22}\beta_{mj} &= -d_{23}. \end{aligned} \tag{11}$$

If the model of an incompressible fluid is used, the sound speed in a fluid is infinitely large and, respectively, $\tilde{\gamma} = 0$. Moreover, in this case it is possible to replace a ratio between Bessel function J_m and its first derivative by an asymptotic expansion in its small argument and retain only the first term. It gives the following simplified formulation of the element d_{33}:

$$d_{33} = 1 + \frac{h^2}{12R^2} k^4 - \frac{h^2}{12R^2} 2m^2 k^2 + \frac{h^2}{12R^2} m^4 - \Omega^2 - \tilde{\rho}\Omega^2 \frac{R}{h} \frac{1}{m}. \tag{12}$$

This simplification is very important from a computational viewpoint, because it reduces the dispersion equation for a fluid-filled shell to a polynomial form. Apparently, it is not applicable at $m = 0$ because a ratio between Bessel function J_0 and its first derivative in its small argument limit needs to be re-formulated as compared with the case $m \neq 0$. Physically, Eq. (12) becomes non-applicable at $m = 0$ due to the presence of a 'fluid-originated' propagating wave, which co-exists in a fluid-filled shell with a 'structure-originated' one at an arbitrary low frequency.

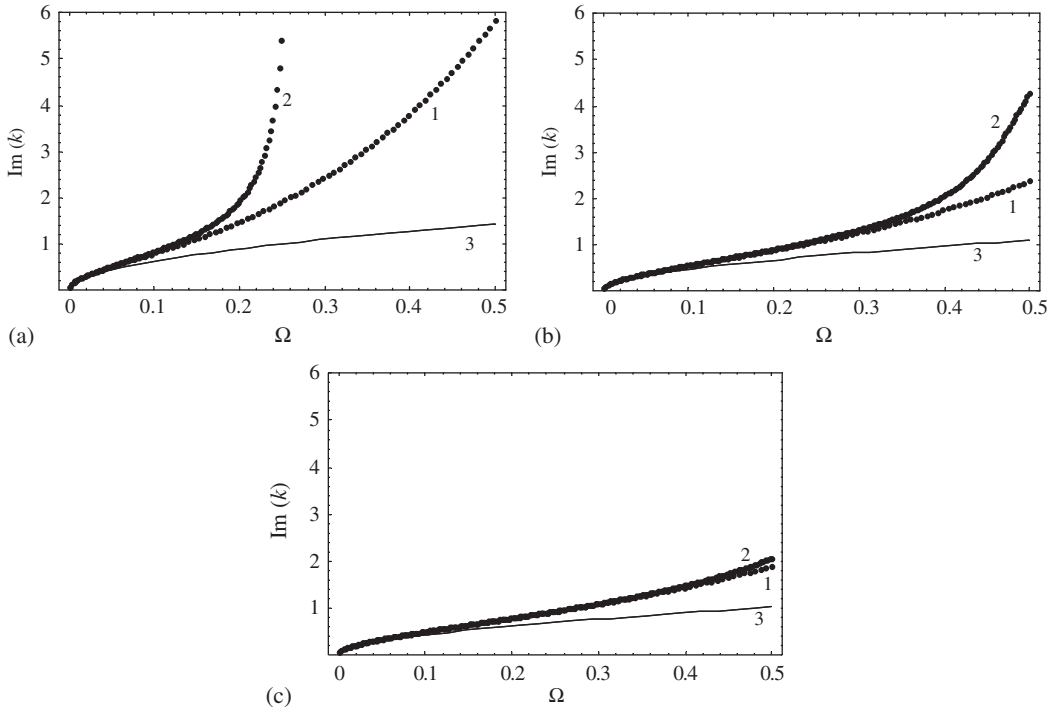

Fig. 2. Dispersion curves for a uniform shell with fluid loading: (a) $h/R = 0.01$, (b) $h/R = 0.05$ and (c) $h/R = 0.1$. Curve 1—the exact theory, curve 2—the simplified theory and curve 3—the beam theory.

If the theory of beam-type motions is used, a fluid is considered as incompressible and a small argument asymptotic is used, then the dispersion equation is reduced as

$$\left(1+\frac{h^2}{12R^2}\right)k^4+\Omega^2k^2-2\Omega^2-\tilde{\rho}\Omega^2\frac{R}{h}=0. \tag{13}$$

As follows from this equation, a fluid simply contributes to the inertial properties of a tube so that particles of the fluid exactly follow transverse motions of a tube at each cross-section as a purely inertial inclusion, which has no stiffness.

The dispersion curves, which describe propagating waves ($\mathrm{Re}(k) = 0$, $\mathrm{Im}(k) > 0$—wave propagates from the left to the right) obtained by use of the exact theory (9), are shown in Fig. 2 by curve 1. Curve 2 in these graphs is plotted after the simplified theory, when formula (12) is substituted in Eq. (9), whereas curve 3 displays a dependence of the wavenumber upon the frequency parameter Ω suggested by dispersion equation (13). As is seen, simplified theories are valid in a broader frequency range, when a shell becomes thicker. For instance, consider a steel shell ($E = 2 \times 10^5$ MPa, $\rho = 7800$ kg/m^3, $\nu = 0.3$) of the radius of $R = 50$ mm. If its thickness is $h = 0.5$ mm, then the model of an incompressible fluid is valid up to approximately $f_{\mathrm{inc}} \approx 3$ kHz and the beam model is valid up to $f_{\mathrm{beam}} \approx 1$ kHz. For a shell of the thickness $h = 2.5$ mm these frequencies are $f_{\mathrm{inc}} \approx 6.5$ kHz and $f_{\mathrm{beam}} \approx 2$ kHz. For a shell of $h = 5$ mm, they are $f_{\mathrm{inc}} \approx 8.5$ kHz and $f_{\mathrm{beam}} \approx 3$ kHz. Thus, it is practical to use the simplified theories to study wave propagation in pipes in a not-too-high-frequency range.

Generally, validity ranges of the simplified theories should be estimated also with respect to description of non-propagating waves (which control the 'near-field' effects). The simplified theories cannot be accurate in a near field, simply because an infinitely large number of so-called 'fluid-originated' modes (see, for example, Ref. [3]) are ignored as soon as the asymptotic formula replaces the ratio of Bessel function to its derivative in the formula for d_{33}. However, both these theories are valid to describe phenomena of the energy transmission. Inasmuch as wave propagation is studied in the present paper, all results reported in subsequent sections for the beam-type mode $m = 1$ are obtained in frameworks of both the simplified theories.

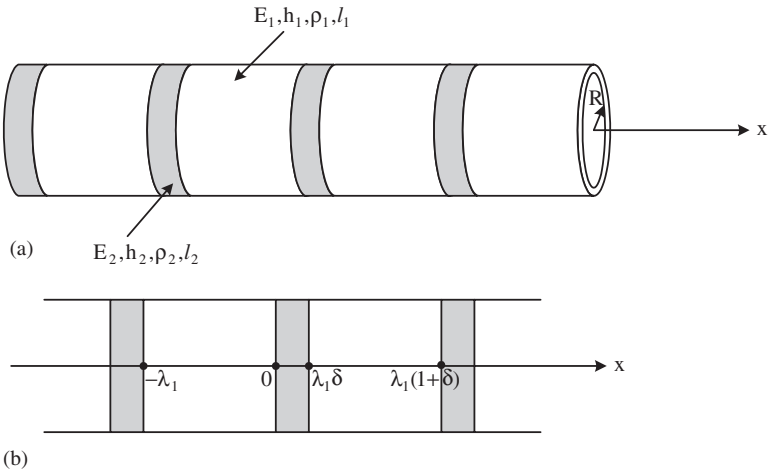

Fig. 3. The periodic infinitely long cylindrical shell: (a) general layout and (b) continuity and periodicity conditions.

3. Analysis of wave propagation in an infinitely long periodic cylindrical shell by use of Floquet theory

An infinitely long cylindrical shell is composed of the set of periodically repeated elements of two types as shown in Fig. 3a. Each set of elements ($j = 1, 2$) is specified by the following parameters: the thickness h_j, the radius R_j, the length l_j, Young's modulus E_j, the density ρ_j, Poisson ratio v_j. Hereafter, it is assumed that $R_1 = R_2 = R$, $v_1 = v_2 \equiv v = 0.3$. It is convenient to introduce the non-dimensional parameters

$$\Omega = \sqrt{\frac{(1-v^2)\rho_1 R^2\omega^2}{E_1}}, \quad \lambda_1 = \frac{l_1}{R}, \quad \delta = \frac{l_2}{l_1}, \quad \alpha = \frac{h_2}{h_1}, \quad \beta = \frac{\rho_2}{\rho_1}, \quad \chi = \frac{E_2}{E_1}.$$

Fluid loading is defined by the parameter $\beta_{\mathrm{fl}} = \rho_{\mathrm{fl}}/\rho_1$. Two theories outlined in the previous section are used to determine location of the frequency band gaps in a periodic cylindrical shell vibrating in the non-axisymmetric mode $m \neq 0$.

3.1. The shell theory

A solution for equations of dynamics of each element of a shell (1) is sought in the form

$$u_{mj}(x) = \sum_{n=1}^{8} A_{mnj}\exp(k_{mnj}x),$$
$$v_{mj}(x) = \sum_{n=1}^{8} B_{mnj}\exp(k_{mnj}x),$$
$$w_{mj}(x) = \sum_{n=1}^{8} C_{mnj}\exp(k_{mnj}x), \quad j = 1, 2. \tag{14}$$

These formulas present an exact solution of the simplified equations (1). Therefore, the contribution of a fluid is reduced to the added mass effect (the asymptotic formula (12) is used) and the dispersion equation for a fluid-filled shell is a polynomial of the same order as for an empty shell.

The wavenumbers are found from the dispersion equation (9) for each segment of a shell and for each individual root of these equations, modal coefficients (10) are found, which define a ratio between amplitudes of the axial, the circumferential and the radial displacements. There are 16 unknown modal amplitudes in formula (14). They are uniquely defined by the continuity and the periodicity conditions, formulated (see also Ref. [3] for details) for axial displacements u_{mj}, circumferential displacements v_{mj}, radial displacements w, slopes w', axial forces Q_{1mj}, circumferential forces Q_{2mj}, transverse forces Q_{3mj} and bending moments Q_{4mj}.

Specifically, the continuity conditions at junction points $x = 0$ and $\lambda_1\delta$ (see Fig. 3b) are:

$$\begin{aligned} &u_{m1}(0) = u_{m2}(0), && v_{m1}(0) = v_{m2}(0),\\ &w_{m1}(0) = w_{m2}(0), && w'_{m1}(0) = w'_{m2}(0),\\ &Q_{1m1}(0) = \chi\alpha Q_{1m2}(0), && Q_{2m1}(0) = \chi\alpha Q_{2m2}(0),\\ &Q_{3m1}(0) = \chi\alpha^3 Q_{3m2}(0), && Q_{4m1}(0) = \chi\alpha^3 Q_{4m2}(0), \end{aligned} \tag{15a}$$

$$\begin{aligned} &u_{m1}(\lambda_1\delta) = u_{m2}(\lambda_1\delta), && v_{m1}(\lambda_1\delta) = v_{m2}(\lambda_1\delta),\\ &w_{m1}(\lambda_1\delta) = w_{m2}(\lambda_1\delta), && w'_{m1}(\lambda_1\delta) = w'_{m2}(\lambda_1\delta),\\ &Q_{1m1}(\lambda_1\delta) = \chi\alpha Q_{1m2}(\lambda_1\delta), && Q_{2m1}(\lambda_1\delta) = \chi\alpha Q_{2m2}(\lambda_1\delta),\\ &Q_{3m1}(\lambda_1\delta) = \chi\alpha^3 Q_{3m2}(\lambda_1\delta), && Q_{4m1}(\lambda_1\delta) = \chi\alpha^3 Q_{4m2}(\lambda_1\delta). \end{aligned} \tag{15b}$$

The same continuity conditions should also hold at all other junction points, $x = n(\delta + 1)\lambda_1$, $n = 0,1,2,\ldots$.

Floquet theory is applied to formulate the periodicity conditions (see Fig. 3b)

$$\begin{aligned} u_{m1}(\delta\lambda_1) &= u_{m1}(-\lambda_1)\exp(\mathrm{i}K_B),\\ v_{m1}(\delta\lambda_1) &= v_{m1}(-\lambda_1)\exp(\mathrm{i}K_B),\\ w_{m1}(\delta\lambda_1) &= w_{m1}(-\lambda_1)\exp(\mathrm{i}K_B),\\ w'_{m1}(\delta\lambda_1) &= w'_{m1}(-\lambda_1)\exp(\mathrm{i}K_B),\\ Q_{nm1}(\delta\lambda_1) &= Q_{nm1}(-\lambda_1)\exp(\mathrm{i}K_B), \quad n = 1,2,3,4. \end{aligned} \tag{16}$$

These conditions are substituted to Eq. (15b) and a system of 16 homogeneous equations with respect to two sets of modal amplitudes C_{mnj}, $n = 1,2,\ldots,8$, $j = 1,2$ is formulated. This system is rather cumbersome and therefore not presented here. It has a non-trivial solution when its determinant vanishes. This condition formulates a transcendental equation with respect to Bloch parameter K_B, which is a standard variable in the subject, measuring a phase shift in a periodic wave-guide [4,5]. The characteristic equation is obtained by equating to zero the dispersion relation formulated in terms of the frequency parameter Ω and Bloch parameter K_B,

$$D(\Omega, K_B) = 0. \tag{17}$$

Then one may formulate either a direct problem of solving the characteristic equation (17)—to find Bloch parameter for a given Ω, or an inverse problem—to find the frequency parameters for a given K_B. As follows from Floquet theory, wave propagation in a periodic structure is possible only when the characteristic equation has at least one purely real root K_B for a given Ω. Thus, only these roots should be determined and it is sufficient to consider the interval $0 < K_B < \pi$ due to the periodicity of the function $\exp(\mathrm{i}K_B)$. The characteristic equation (17) for alternating cylindrical segments cannot be explicitly formulated as $\Omega(K_B) = 0$. Thus, the direct problem should be solved—to find from Eq. (17) a value of Bloch parameter K_B in the interval $0 < K_B < \pi$ for a given Ω and to plot branches $K_B(\Omega)$ one by one.

3.2. Beam theory, $m = 1$

In the framework of this theory, general solution of Eq. (13) is sought as

$$w_{1j}(x) = \sum_{n=1}^{4} C_{1nj}\exp(\mathrm{i}k_{1nj}x), \quad j = 1,2. \tag{18}$$

The dispersion equation for each segment of a tube is formulated as Eq. (13). Matching conditions at the interfaces $x = 0$ and $\lambda_1\delta$ are formulated as the continuity of displacements w_{1j}, slopes w'_{1j}, bending moments Q_{14j} and transverse forces Q_{13j} in the non-dimensional form

$$\begin{aligned} &w_{11}(0) = w_{12}(0), && w'_{11}(0) = w'_{12}(0),\\ &Q_{311}(0) = \chi\alpha^3 Q_{312}(0), && Q_{411}(0) = \chi\alpha^3 Q_{412}(0), \end{aligned} \tag{19a}$$

$$\begin{aligned} &w_{11}(\lambda_1\delta) = w_{12}(\lambda_1\delta), \qquad w'_{11}(\lambda_1\delta) = w'_{12}(\lambda_1\delta),\\ &Q_{311}(\lambda_1\delta) = \chi\alpha^3 Q_{312}(\lambda_1\delta), \quad Q_{411}(\lambda_1\delta) = \chi\alpha^3 Q_{412}(\lambda_1\delta). \end{aligned} \tag{19b}$$

The same conditions are also applied at all other junction points $x = n\lambda_1(1+\delta)$, $n = 0, 1, 2, \ldots$.

Floquet theory [4,5] is used to formulate the periodicity conditions

$$\begin{aligned} &w_{11}(\delta\lambda_1) = w_{11}(-\lambda_1)\exp(\mathrm{i}K_B),\\ &w'_{11}(\delta\lambda_1) = w'_{11}(-\lambda_1)\exp(\mathrm{i}K_B),\\ &Q_{311}(\delta\lambda_1) = Q_{311}(-\lambda_1)\exp(\mathrm{i}K_B),\\ &Q_{411}(\delta\lambda_1) = Q_{411}(-\lambda_1)\exp(\mathrm{i}K_B). \end{aligned} \tag{20}$$

These conditions are substituted in Eq. (19b) and a system of eight homogeneous equations with respect to eight modal amplitudes grouped in two sets, A_{nj}, $n = 1, 2, 3, 4$, $j = 1, 2$ is derived. Then similarly to the previous case, Eq. (17) is solved with respect to Bloch parameter K_B.

It is appropriate to begin with analysis of the mechanism of generation of band gaps, when elements of an infinite periodic shell depart from being of identical properties. This analysis is performed in the framework of a shell theory for the following set of parameters: $\alpha = 1$, $\beta = 1$, $\lambda_1 = 2$, $\delta = 0.2$, $h/R = 0.05$, $m = 1$, $\beta_{\mathrm{fl}} = 0$. In Fig. 4a, characteristic curves $\Omega(K_B)$ are plotted for a uniform shell (i.e., for $\chi = 1$). As is seen they constitute a continuous 'ladder' without band gaps. Moreover, at relatively high frequencies ($\Omega > 0.6$), two characteristic curves exist simultaneously, which specify two propagating waves with different phases. As soon as a discontinuity in the properties of shell elements is introduced, a continuous 'ladder' disappears, as shown in Fig. 4b plotted for $\chi = 0.5$. In this case, the difference in properties of the elements is relatively small, but two frequency band gaps are already generated, $0.42 < \Omega < 0.48$ and $0.65 < \Omega < 0.685$. The mechanism of their generation is different: the former one is produced due to a discontinuity in the 'swap' from the first to the second branch at $K_B = \pi$, whereas the second one is generated in vicinity of the intersection point of the second and the third branches of characteristic curve for a uniform shell. Curves in Fig. 4c are plotted for $\chi = 0.1$. The first branch has a smaller slope than in the two previous cases, but its location is not altered

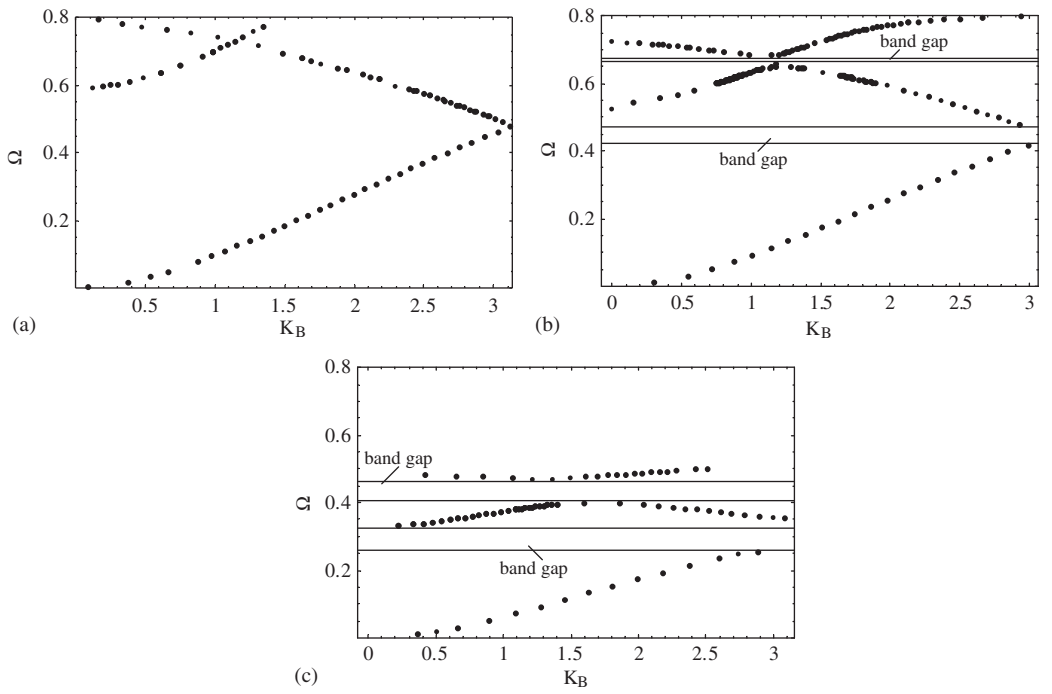

Fig. 4. Transformations of characteristic curves with variation in the parameter χ (shell theory): (a) $\chi = 1$, (b) $\chi = 0.5$ and (c) $\chi = 0.1$.

significantly. The second and the third branches are transformed to almost straight lines and they are substantially pulled down from their counterparts. Therefore the first and the second band gaps are located at $0.26<\Omega<0.354$ and $0.4<\Omega<0.475$. At higher frequencies ($\Omega>0.5$), there are several other characteristic curves, which are extended from $K_B=0$ to $K_B=\pi$, each in a very narrow frequency pass band, but they are not presented in Fig. 4.

The results, obtained in the framework of the shell theory and the beam theory, are summarized in Figs. 5–9. In all graphs, characteristic curves $\Omega(K_B)$, which present a dependence of the frequency parameter on the purely real Bloch parameter, obtained in the framework of a shell theory are plotted by dotted lines. In Figs. 5–7, the same dependence predicted by the elementary theory (which is valid only for $m=1$) is presented by solid lines. All graphs are extended in Bloch parameter in the interval $(0,\pi)$ due to the natural periodicity of the exponent of a purely imaginary argument. The upper limit in a frequency range is controlled by the applicability of the both theories, which has been estimated in the previous section.

The graphs in Fig. 5 are plotted for a shell with the following parameters: $\alpha=1$, $\beta=1$, $\lambda_1=2$, $\delta=0.2$, $\chi=0.01$, $h/R=0.05$, $m=1$, no fluid loading. The frequency band gap predicted by the elementary beam theory ($0.148<\Omega<0.589$) is broader than its counterpart predicted by the shell theory, which is actually split into three segments ($0.097<\Omega<0.112$, $0.146<\Omega<0.216$, $0.219<\Omega<0.471$). Narrow pass bands ($0.112<\Omega<0.146$, $0.216<\Omega<0.219$) are not captured at all by the beam theory. The pattern of characteristic curves obtained by use of the shell theory is much more complicated than in the beam theory and it is somewhat similar to the one observed in Ref. [3] for the axisymmetric vibrations (it should be noted that the circumferential displacement is also involved in wave motion at $m=1$). Nevertheless, the beam theory gives a reasonably good 'initial guess' for the location of the first frequency band gap.

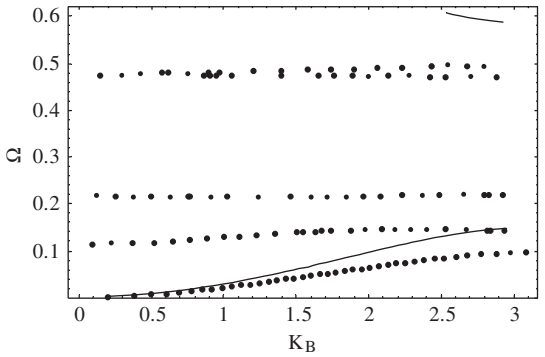

Fig. 5. Comparison of characteristic curves ('thin' shell, no fluid loading). Dotted curves—the shell theory and continuous curves—the beam theory.

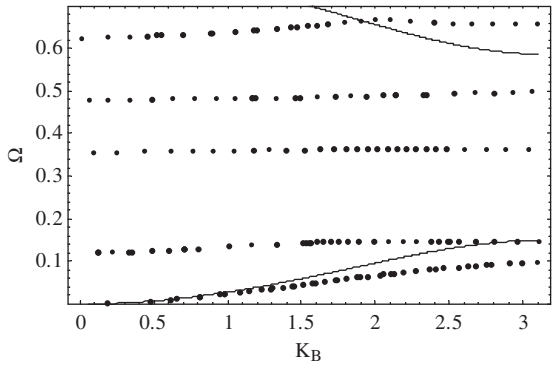

Fig. 6. Comparison of characteristic curves ('thick' shell, no fluid loading). Dotted curves—the shell theory and continuous curves—the beam theory.

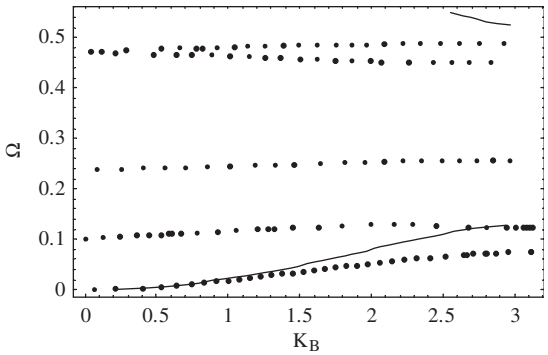

Fig. 7. Comparison of characteristic curves ('thick' shell, fluid loading). Dotted curves—the shell theory and continuous curves—the beam theory.

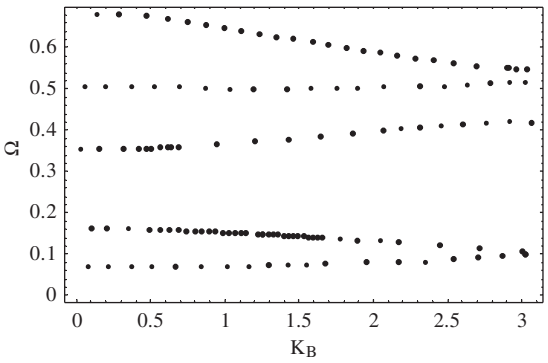

Fig. 8. Characteristic curves (shell theory, 'thick' shell, $m = 2$, no fluid loading).

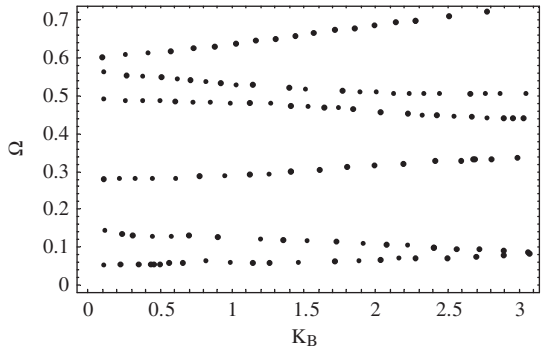

Fig. 9. Characteristic curves (shell theory, 'thick' shell, $m = 2$, fluid loading).

In the case of a thicker shell, $h/R = 0.1$ (all other parameters are not altered), the prediction of the beam theory agrees with the shell theory better than in the previous case as is seen in Fig. 6. Similarly to the previous case, the shell theory predicts three narrow pass bands ($0.126 < \Omega < 0.148$, $0.361 < \Omega < 0.365$, $0.4948 < \Omega < 0.495$), which split the frequency band gap $0.0952 < \Omega < 0.629$ into four segments. However, the lower boundary of the band gap is rather satisfactory predicted by the beam theory as $\Omega = 0.15$. The upper boundary is underestimated by the beam theory, $\Omega = 0.586$. This result appears to be rather obvious inasmuch in the low-frequency range the behaviour of a thick shell is adequately approximated by the behaviour of a beam of tubular cross-section. The effect of heavy fluid loading ($\beta_{fl} = 0.128$) is illustrated in Fig. 7 for a shell

with the same parameters as in the previous case. The first three frequency band gaps predicted by the shell theory are located in $0.075<\Omega<0.101$, $0.125<\Omega<0.241$ and $0.258<\Omega<0.45$, whereas the beam theory suggests the single band gap in $0.128<\Omega<0.526$. As is seen from this figure, characteristic curves predicted by the shell theory are pulled down in a frequency domain more significantly, than their counterparts obtained by use of the beam theory. The lower boundary of the first frequency band gap is overestimated, several narrow pass bands are not captured at all and the upper boundary of the stop band is also overestimated by the beam theory.

Finally, the wave propagation in an infinitely long periodic shell with ($\beta_{\mathrm{fl}}=0.128$) and without ($\beta_{\mathrm{fl}}=0$) heavy fluid loading at the circumferential wavenumber $m=2$ is addressed. The parameters of a shell are $\alpha=1$, $\beta=1$, $\lambda=2$, $\delta=0.2$, $\chi=0.01$, $h/R=0.1$. Computations are performed only by use of the shell theory. In Figs. 8 and 9, the characteristic curves (dotted lines) are shown for the shell without and with fluid loading, respectively. The distinctive feature of these graphs is an existence of the cutoff frequency ($\Omega_{\mathrm{cuton}}\approx 0.071$ for a shell without heavy fluid loading; $\Omega_{\mathrm{cuton}}\approx 0.055$ for a shell with heavy fluid loading). These graphs are extended to somewhat higher frequencies, than their counterparts at $m=1$, because the validity range of the model of an incompressible fluid extends with a growth in the circumferential wavenumber. As is seen in Fig. 8, the first three frequency band gaps for an empty shell are located at $0.161<\Omega<0.356$, $0.42<\Omega<0.5$ and $0.513<\Omega<0.548$. In the presence of heavy fluid loading these band gaps are transformed to $0.133<\Omega<0.279$, $0.335<\Omega<0.439$ and $0.484<\Omega<0.506$, see Fig. 9.

To conclude this brief discussion of the 'frequency band gaps' predicted by the two theories, it can be pointed out that the beam theory is reliably applicable only for sufficiently thick shells and only to identify the lower boundary of the first band gap. In general, it overestimates the size of a band gap. This observation has an elementary physical explanation—the beam theory is set up when the kinematical constraints (3) are imposed. Thus, several types of wave motions, which are admissible in a shell, are excluded from consideration in the beam theory. If these types of wave motion may develop only in a relatively high-frequency range, then an error of the beam theory is insignificant. Otherwise, it becomes quite large.

4. Boundary equations for a cylindrical shell under internal heavy loading

Results reported in the previous section are obtained for the idealized model of a periodic structure composed of an infinite set of alternating elements. Apparently, in any practical case it is possible to insert just a few elements into a pipe and it is necessary to check whether a significant reduction in the energy injected into the fluid-filled shell (which is conveniently measured by an input mobility, or by the imaginary part of the amplitude of displacement at a point, where the excitation force is applied) is achieved. Then the problem in forced vibrations of a non-uniform cylindrical shell should be solved. This solution in an exact form is readily available from the methodology of boundary equations [7].

The exact formulation of boundary equations for a cylindrical shell filled with an acoustic medium involves Somigliana identities for an acoustic variable (a velocity potential) as well as for shell variables (components of displacements). However, in the reduced formulation of dynamics of a shell under heavy fluid loading (when the dispersion equation for a shell under heavy internal fluid loading is a polynomial of the same order, as for an empty shell), the identities for a fluid should be thought of as a consequence of those for a structure, specifically, formulated for a radial displacement. The detailed derivation of Somigliana identities for an empty shell is available in Ref. [7]. They are formulated as

$$\begin{aligned} u_m(\xi) = {} & \left[Q_{1m}(x)u_m^{01}(x,\xi) + Q_{2m}(x)v_m^{01}(x,\xi) + Q_{3m}(x)w_m^{01}(x,\xi) + Q_{4m}(x)\frac{\partial w_m^{01}(x,\xi)}{\partial x} \right]\Big|_{x=0}^{x=l} \\ & - \left[Q_{1m}^{01}(x,\xi)u_m(x) + Q_{2m}^{01}(x,\xi)v_m(x) + Q_{3m}^{01}(x,\xi)w_m(x) + Q_{4m}^{01}(x,\xi)\frac{\mathrm{d}w_m(x)}{\mathrm{d}x} \right]\Big|_{x=0}^{x=l} \\ & + \int_0^l \left[q_{1m}(x)u_m^{01}(x,\xi) + q_{2m}(x)v_m^{01}(x,\xi) + q_{3m}(x)w_m^{01}(x,\xi) \right]\mathrm{d}x \end{aligned} \tag{21a}$$

$$v_m(\xi) = \left[Q_{1m}(x)u_m^{02}(x,\xi) + Q_{2m}(x)v_m^{02}(x,\xi) + Q_{3m}(x)w_m^{02}(x,\xi) + Q_{4m}(x)\frac{\partial w_m^{02}(x,\xi)}{\partial x} \right]\Big|_{x=0}^{x=l}$$
$$- \left[Q_{1m}^{02}(x,\xi)u_m(x) + Q_{2m}^{02}(x,\xi)v_m(x) + Q_{3m}^{02}(x,\xi)w_m(x) + Q_{4m}^{02}(x,\xi)\frac{\mathrm{d}w_m(x)}{\mathrm{d}x} \right]\Big|_{x=0}^{x=l}$$
$$+ \int_0^l \left[q_{1m}(x)u_m^{02}(x,\xi) + q_{2m}(x)v_m^{02}(x,\xi) + q_{3m}(x)w_m^{02}(x,\xi) \right]\mathrm{d}x, \tag{21b}$$

$$w_m(\xi) = \left[Q_{1m}(x)u_m^{03}(x,\xi) + Q_{2m}(x)v_m^{03}(x,\xi) + Q_{3m}(x)w_m^{03}(x,\xi) + Q_{4m}(x)\frac{\partial w_m^{03}(x,\xi)}{\partial x} \right]\Big|_{x=0}^{x=l}$$
$$- \left[Q_{1m}^{03}(x,\xi)u_m(x) + Q_{2m}^{03}(x,\xi)v_m(x) + Q_{3m}^{03}(x,\xi)w_m(x) + Q_{4m}^{03}(x,\xi)\frac{\mathrm{d}w_m(x)}{\mathrm{d}x} \right]\Big|_{x=0}^{x=l}$$
$$+ \int_0^l \left[q_{1m}(x)u_m^{03}(x,\xi) + q_{2m}(x)v_m^{03}(x,\xi) + q_{3m}(x)w_m^{03}(x,\xi) \right]\mathrm{d}x, \tag{21c}$$

$$\frac{\mathrm{d}w_m(\xi)}{\mathrm{d}\xi} = \left[Q_{1m}(x)\frac{\partial u_m^{03}(x,\xi)}{\partial \xi} + Q_{2m}(x)\frac{\partial v_m^{03}(x,\xi)}{\partial \xi} + Q_{3m}(x)\frac{\partial w_m^{03}(x,\xi)}{\partial \xi} + Q_{4m}(x)\frac{\partial^2 w_m^{03}(x,\xi)}{\partial \xi \partial x} \right]\Big|_{x=0}^{x=l}$$
$$- \left[\frac{\partial Q_{1m}^{03}(x,\xi)}{\partial \xi}u_m(x) + \frac{\partial Q_{2m}^{03}(x,\xi)}{\partial \xi}v_m(x) + \frac{\partial Q_{3m}^{03}(x,\xi)}{\partial \xi}w_m(x) + \frac{\partial Q_{4m}^{03}(x,\xi)}{\partial \xi}\frac{\mathrm{d}w_m(x)}{\mathrm{d}x} \right]\Big|_{x=0}^{x=l}$$
$$+ \int_0^l \left[q_{1m}(x)\frac{\partial u_m^{03}(x,\xi)}{\partial \xi} + q_{2m}(x)\frac{\partial v_m^{03}(x,\xi)}{\partial \xi} + q_{3m}(x)\frac{\partial w_m^{03}(x,\xi)}{\partial \xi} \right]\mathrm{d}x. \tag{21d}$$

In these identities, elements of Green's matrix $u_m^{0j}(x,\xi)$, $v_m^{0j}(x,\xi)$, $w_m^{0j}(x,\xi)$, $Q_{nm}^{0j}(x,\xi)$, $n = 1,2,3,4$, $j = 1,2,3$ are introduced as solutions of a problem of wave propagation in a cylindrical shell in three 'fundamental' loading cases—an excitation by the axial unit force, by the circumferential unit force and by the radial unit force. Each of these forces is concentrated as a δ-function at the point ξ in the axial direction and distributed as a sinusoidal function along the circumference of a shell. Right-hand sides of these equations contain driving distributed forces in the axial, circumferential and radial direction $q_{1m}(x)$, $q_{2m}(x)$, $q_{3m}(x)$. They should be set to zero in the cases, when propagation of free waves in an infinitely long shell and free vibrations of a shell of the finite length are concerned.

Four Eqs. (21) contain 16 unknown values of boundary displacements and generalized forces at the edges of a shell. Respectively, eight boundary equations are obtained by putting an observation point at the edge $x = 0$ and at the edge $x = l$. For a shell of a finite length, the boundary conditions are formulated at the edges $x = 0, l$ as

$$\begin{aligned} &\chi_{11}Q_{1m} + \chi_{12}u_m = 0,\\ &\chi_{21}Q_{2m} + \chi_{22}v_m = 0,\\ &\chi_{31}Q_{3m} + \chi_{32}w_m = 0,\\ &\chi_{41}Q_{4m} + \chi_{42}\frac{\mathrm{d}w_m}{\mathrm{d}x} = 0, \end{aligned} \tag{22a}$$

$$\begin{aligned} &\chi_{51}Q_{1m} + \chi_{52}u_m = 0,\\ &\chi_{61}Q_{2m} + \chi_{62}v_m = 0,\\ &\chi_{71}Q_{3m} + \chi_{72}w_m = 0,\\ &\chi_{81}Q_{4m} + \chi_{82}\frac{\mathrm{d}w_m}{\mathrm{d}x} = 0. \end{aligned} \tag{22b}$$

An arbitrary set of conditions may be modelled by an appropriate choice of the coefficients χ_{ij}, $i = 1,2,\ldots,8$, $j = 1,2$ (for example, the set $\chi_{i2} = 0$, $i = 1,2,\ldots,8$ defines an unconstrained shell). Then a system of algebraic

Table 1

Boundary conditions	$h/R = 0.01$		$h/R = 0.05$		$h/R = 0.1$	
	$\beta = 0$	$\beta = 0.128$	$\beta = 0$	$\beta = 0.128$	$\beta = 0$	$\beta = 0.128$
$x = 0, L$	0.845	0.232	0.857	0.463	0.894	0.601
$Q_1 = v = w = Q_4 = 0$	1.986	0.455	1.987	0.581	1.991	0.986
$x = 0, L$	0.855	0.346	0.911	0.493	1.063	0.717
$u = v = w = w' = 0$	1.284	0.413	1.290	0.685	2.016	1.339
$x = 0$	0.553	0.171	0.562	0.332	0.575	0.415
$u = v = w = w' = 0$						
$x = L$	0.953	0.299	0.966	0.515	1.114	0.743
$Q_1 = Q_2 = Q_3 = Q_4 = 0$						

equations (21)–(22) is composed, which uniquely defines the amplitudes of forced vibrations of a cylindrical shell of a finite length. This system can also be conveniently used to determine the eigenfrequencies of a fluid-filled shell of a finite length with arbitrary boundary conditions. Inasmuch the elements of Green's matrix are derived with the use of a simplified model of fluid loading, the formulation of structural boundary conditions at the edges automatically defines the boundary conditions for a fluid or rather some 'equivalent' condition.

In Table 1, the first and the second non-dimensional eigenfrequency Ω of a uniform cylindrical shell with and without fluid inside are presented for three sets of boundary conditions and three magnitudes of a thickness-to-radius ratio. The non-dimensional length of a shell is $l = 1$ (i.e., the length is equal to the radius). As follows from this table, eigenfrequencies become substantially lower due to the significant added mass effect. It is particularly noticeable for a thin shell of $h/R = 0.01$. Its eigenfrequencies decrease much more, than those of a thick shell, $h/R = 0.1$. This is a rather obvious result inasmuch a ratio of the mass of water inside a shell to the mass of a shell is proportional to R/h. However, it should be pointed out that such a simple behaviour is typical for the first and the second natural frequencies in the beam-type spectrum, $m = 1$. Some of the higher eigenfrequencies at $m = 1$ are related to predominantly tangential modes and the influence of fluid loading is weaker. In the 'breathing mode', $m = 0$, the fluid may produce the effect of an added stiffness, rather than an added mass effect.

5. Formulation of boundary equations for a semi-infinite cylindrical shell composed of alternating segments

The methodology of boundary equations is readily applicable for analysis of wave propagation in a non-uniform cylindrical shell with and without heavy fluid loading composed of several alternating elements. As is discussed in Section 1, the problem of considerable practical interest is to explore a possibility to reduce the energy input into a shell under heavy internal fluid loading by use of small number of alternating elements. Consider a semi-infinite cylindrical shell clamped at the edge $x = 0$

$$u_m = 0, \quad v_m = 0, \quad w_m = 0, \quad \frac{\mathrm{d}w_m}{\mathrm{d}x} = 0. \tag{23}$$

This shell is loaded by, say, a unit radial force, which is concentrated in the axial direction at $x = x_0$ and distributed as a sinusoidal function along the circumference of a shell, i.e., $q_{1m}(x) = q_{2m}(x) = 0$, $q_{3m}(x) = \delta(x - x_0)$. The injected and transmitted power for a real-valued excitation is only related to the imaginary part of the receptance, (in the case of excitation by a radial force), i.e., to $\mathrm{Im}(w_m(x_0))$.

If a shell is homogeneous, then this force injects the energy at any excitation frequency ($m = 1$) and above some cutoff frequency ($m > 1$). However, if a shell is composed of alternating elements, then its response to the driving force should be rather different depending on whether the excitation frequency lies inside or outside frequency band gaps predicted by Floquet theory. Apparently, it is not feasible to introduce an infinite number of the alternating elements in any industrial pipeline and the complete suppression of the wave propagation

does not seem to be possible. However, it is highly desirable to achieve maximum possible decrease in the imaginary part of the receptance or (which is the same up to the factor ω) in the input mobility by introduction of just a few alternating elements.

The system of governing linear algebraic equations, which yields the exact solution of the problem contains the following 16 unknowns at each edge of the jth element of a finite length: axial displacements u_{mj}, circumferential displacements v_{mj}, radial displacements w_{mj}, slopes w'_{mj}, axial forces Q_{1mj}, circumferential forces Q_{2mj}, transverse forces Q_{3mj} and axial bending moments Q_{4mj}. Naturally, only eight of these quantities should be determined at the edge of a semi-infinite element. For each element of a finite length, eight boundary equations (21) are available, whereas four boundary equations are formulated for a semi-infinite element. At each junction cross-section $x = x_n$, eight continuity conditions are formulated for the jth and $(j+1)$th element:

$$\begin{aligned} &u_{mj}(x_n) = u_{mj+1}(x_n), && v_{mj}(x_n) = v_{mj+1}(x_n),\\ &w_{mj}(x_n) = w_{mj+1}(x_n), && w'_{mj}(x_n) = w'_{mj+1}(x_n),\\ &Q_{1mj}(x_n) = \chi\alpha Q_{1mj+1}(x_n), && Q_{2mj}(x_n) = \chi\alpha Q_{2mj+1}(x_n),\\ &Q_{3mj}(x_n) = \chi\alpha^3 Q_{3mj+1}(x_n), && Q_{4mj}(x_n) = \chi\alpha^3 Q_{4mj+1}(x_n). \end{aligned} \tag{24}$$

It does not present serious difficulties to formulate the exact solution for an arbitrary number of alternating elements. However, it is practical to consider first some 'primitive' layouts of a structure, which is composed of minimum number of periodicity cells (the pairs of alternating elements).

5.1. The 'four elements' composition

This composition of a non-uniform shell is illustrated in Fig. 10a. Possibly, this is the simplest layout of a structure, because it includes only one cell of periodicity. The system of linear algebraic equations includes eight boundary equations for the first element of the first type, eight boundary equations for the first element of the second type, eight boundary equations for the second element of the first type and four boundary equations for the semi-infinite element of the second type. There are four boundary conditions (23) at the clamped edge and three sets of eight continuity conditions (24) for each of three junctions between the elements. Thus, a system is of the 56th order and it yields an exact solution of the problem.

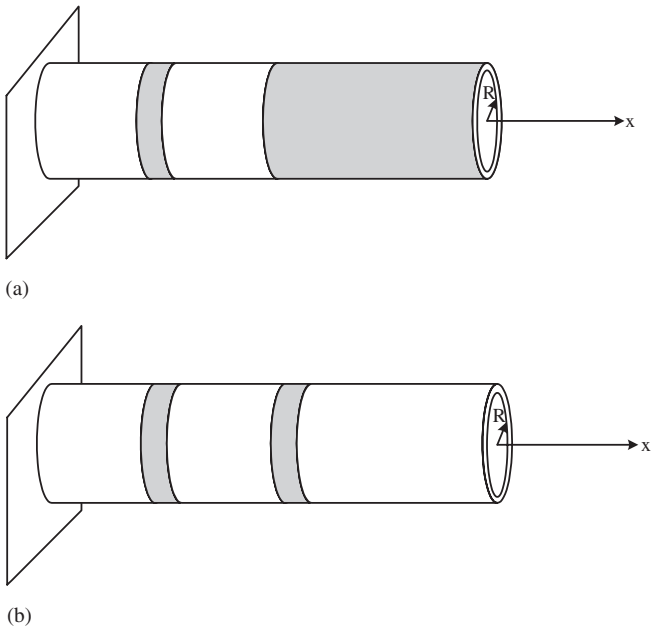

Fig. 10. Non-uniform cylindrical shell: (a) 'Four elements' composition and (b) 'Five elements' composition.

5.2. The 'five elements' composition

The composition of a non-uniform shell is illustrated in Fig. 10b. One more element is added to the set-up displayed in Fig. 10a, and this layout may be described as 'one and a half' or 'two' cells of periodicity layout. In this case a system of linear algebraic equations of the 72nd-order yields an exact solution of the problem.

In the present paper, the analysis of wave propagation in a semi-infinite non-uniform cylindrical shell is performed for these two layouts of this structure. As it will be shown, the results obtained from Floquet theory may be reliably confirmed by comparison with the exact boundary equations solution in these two cases.

6. Input mobilities of a non-uniform shell inside and outside frequency band gaps

In this section, the predictions from Floquet theory (which deals with an infinitely large number of alternating segments) are compared with the solution for a finite number of such elements, specifically, for the 'four elements' and for the 'five elements' compositions of a shell. The point of particular practical interest is to estimate a decrease in the input mobility for the 'generic' excitation case by a radial force.

To judge upon the efficiency of reduction in the input mobility due to the presence of alternating segments, it is appropriate to introduce a 'reference level', which presents the Bloch parameter K_B and the scaled input receptance A (the imaginary part of the non-dimensional amplitude of displacement at the point, where a unit radial force is applied, see discussion in Section 5) versus excitation frequency for a uniform shell. In Fig. 11, these curves are plotted for a shell with $h/R = 0.05$, $m = 1$, $\beta_{\mathrm{fl}} = 0$. Dots present the results from Floquet theory, i.e., $\Omega(K_B)$, continuous curves present the results from the boundary equations method, i.e., $\Omega(K_B)$ (actual calculations are performed to get $A(\Omega)$). As is seen, characteristic curves $\Omega(K_B)$ compose a continuous 'ladder' and wave propagation is possible at any frequency. Similarly, a dependence of the input receptance on the excitation frequency is fairly smooth. It is interesting to note that the maximum in the input receptance is observed exactly at the frequency, characterized by the coincidence of phases of two propagating waves in an infinitely long uniform structure. In subsequent figures, the similar results are presented for a non-uniform shell and the same notations are used.

In Fig. 12a, characteristic curves $\Omega(K_B)$ from Fig. 4 for a shell with $\alpha = 1$, $\beta = 1$, $\lambda = 2$, $\delta = 0.2$, $\chi = 0.01$, $h/R = 0.05$, $m = 1$, $\beta_{\mathrm{fl}} = 0$ are superimposed on curves $\Omega(A)$ for the 'four elements' composition of a shell. As is seen from this graph, the frequency range, where a very sharp drop in the magnitude of the input mobility is detected agrees with the location of the principal band gap predicted by Floquet theory. Some difference between these predictions is observed only in the range $0.11 < \Omega < 0.14$. This picture remains almost the same in the case when the input mobility is computed for the 'five elements' composition of the same shell (see Fig. 12b). Such a small difference between these two graphs suggests that the suppression effect is already achieved with only four elements or, in effect, by use of a single cell of periodicity.

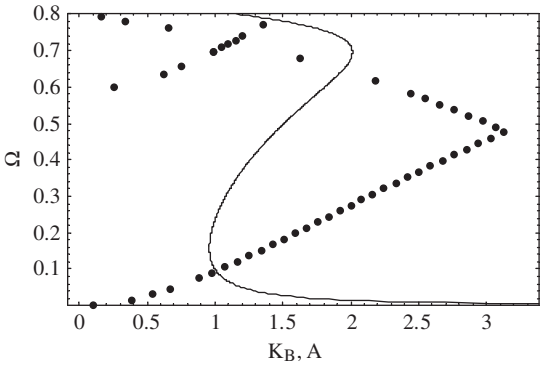

Fig. 11. Characteristic curves (dotted lines, Floquet theory) and scaled input receptance (continuous line, boundary integral equations method) for a uniform shell.

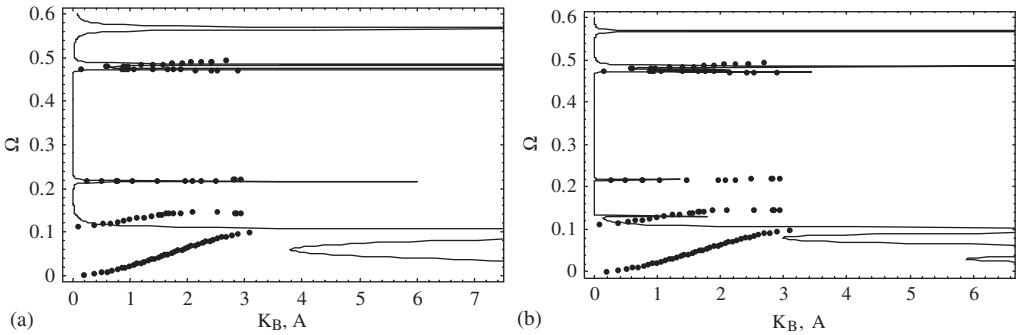

Fig. 12. Characteristic curves (dotted lines) and scaled input receptance (continuous lines) for 'thin' shell, no fluid loading: (a) 'Four elements' composition and (b) 'Five elements' composition.

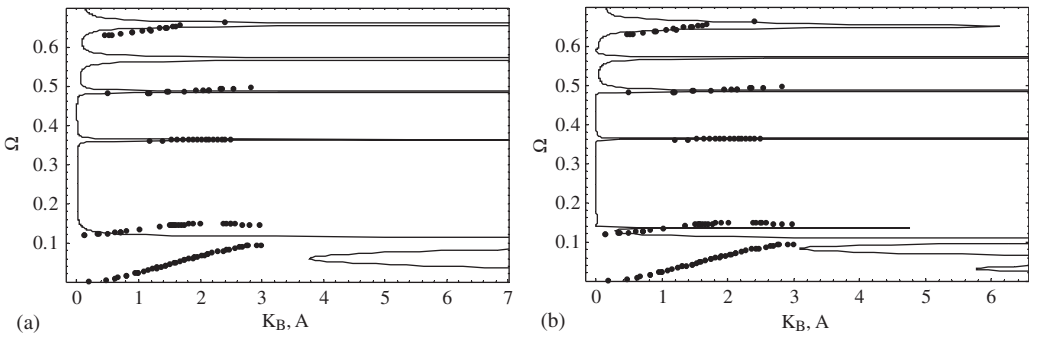

Fig. 13. Characteristic curves (dotted lines) and scaled input receptance (continuous lines) for 'thick' shell, no fluid loading: (a) 'Four elements' composition and (b) 'Five elements' composition.

Graphs in Fig. 13a and b are plotted in the same way as in Fig. 12a and b. The shell parameters are $\alpha = 1$, $\beta = 1$, $\lambda = 2$, $\delta = 0.2$, $\chi = 0.01$, $h/R = 0.1$, $m = 1$, $\beta_{\mathrm{fl}} = 0$. There is also a good agreement between the solution from Floquet theory and the exact solution for the both layouts of a structure. The interesting feature of these graphs is the existence of a very sharp peak in the input mobility, observed at the frequency $\Omega \approx 0.57$ in the solution by boundary equations. The 'original' solution by Floquet theory (see discussion in Section 3) failed to capture this very narrow pass band because a step in the frequency parameter was too coarse. However, the repeated calculations in vicinity of this frequency detected a branch of characteristic curve, which actually looks like an almost straight horizontal line (this branch is not displayed in Fig. 13). Graphs in Fig. 14 are plotted for the same shell with $\beta_{\mathrm{fl}} = 0.128$ and there is no qualitative difference in results obtained for a shell with and without fluid loading. The predictions from Floquet theory capture all the peaks and 'drops' in the input mobility for a shell of 'four elements' and 'five elements' composition and there is a small difference between results obtained for these layouts.

Finally, results for a shell $\alpha = 1$, $\beta = 1$, $\lambda = 2$, $\delta = 0.2$, $\chi = 0.01$, $h/R = 0.1$ without ($\beta_{\mathrm{fl}} = 0$) and with ($\beta_{\mathrm{fl}} = 0.128$) heavy fluid loading at the circumferential wavenumber $m = 2$ are shown in Figs. 15 and 16, respectively. In this case, a decay in the input mobility of a shell is observed in the first frequency band gaps predicted by Floquet theory (as well as in the frequency range below the cutoff frequency). The agreement between these two theories is very good indeed up to the frequency of approximately $\Omega \approx 0.35$ (for a shell without fluid loading) and up to $\Omega \approx 0.29$ (for a shell with fluid loading). At higher frequencies, some discrepancy is observed. The difference between results obtained for a shell of 'four elements' and 'five elements' composition is larger, than in previous cases. Therefore it is possible that a somewhat better agreement may be reached if a shell composed of a larger number of 'periodicity cells' is considered.

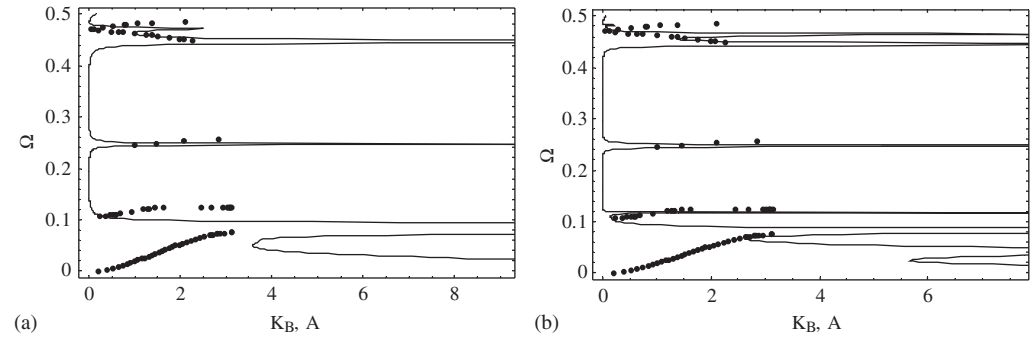

Fig. 14. Characteristic curves (dotted lines) and scaled input receptance (continuous lines) for 'thick' shell, fluid loading: (a) 'Four elements' composition and (b) 'Five elements' composition.

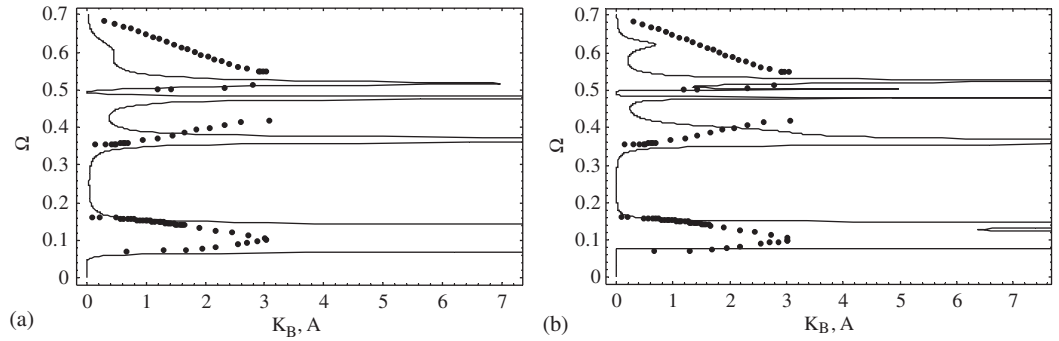

Fig. 15. Characteristic curves (dotted lines) and scaled input receptance (continuous lines) for 'thick' shell, $m = 2$, no fluid loading: (a) 'Four elements' composition and (b) 'Five elements' composition.

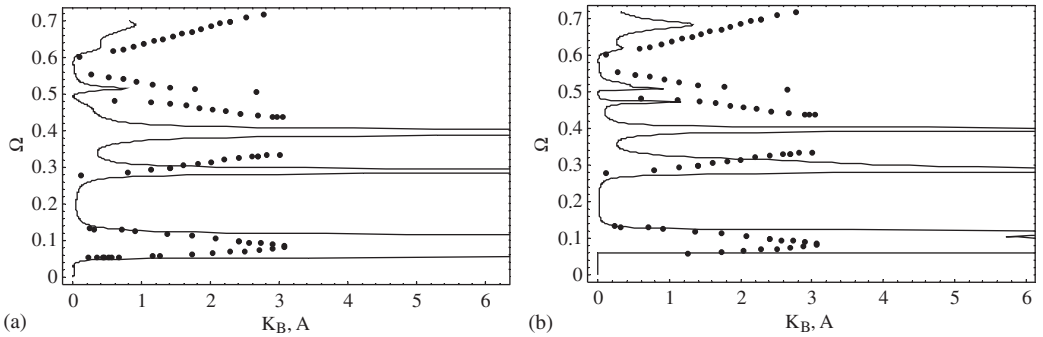

Fig. 16. Characteristic curves (dotted lines) and scaled input receptance (continuous lines) for 'thick' shell, $m = 2$, fluid loading: (a) 'Four elements' composition and (b) 'Five elements' composition.

Summing up results of calculations by the boundary equations method and by Floquet theory it should be noted that their predictions are in a good agreement in all reported examples. It is remarkable that a substantial decrease in the input receptance within a frequency band gap is achieved by means of just a few alternating inclusions. In fact, only one periodicity element is implemented in the 'four element' composition. This result is rather important from the practical viewpoint because such a design modification of a pipeline can be easily implemented. However, it should be pointed out that such a significant suppression of the energy transmission is observed when a relatively long inclusion ($\delta = 0.2$) is inserted into a relatively thick shell. In the

cases, when a 'soft' inclusion is shorter or a shell is thinner, the same decay in the input receptance is achieved with two or three cells of periodicity. Also, the efficiency of suppression of wave propagation is found to be sensitive to the circumferential wavenumber and to the excitation frequency.

7. Conclusions

The investigation reported in this paper addresses several aspects of dynamics of elastic cylindrical shells under internal heavy fluid loading which previously have not been studied in detail. Firstly, Floquet theory is applied to detect the location of frequency band gaps in an infinitely long periodic fluid-filled cylindrical shell vibrating in the 'beam-type' mode $m = 1$ and in the mode $m = 2$, in the framework of two simplified theories. As a prerequisite for this study, the validity range of these theories is estimated by comparison of dispersion curves with those predicted in the exact problem formulation. It is shown that the simplified shell theory is valid for the frequency range of practical interest, whereas the beam theory may be reliably used only for relatively thick shells. Secondly, the boundary integral equations are derived for a cylindrical shell under internal heavy fluid loading and they are applied both for the calculation of eigenfrequencies of a finite shell and for the calculation of energy transmission in a semi-infinite non-uniform shell. The influence of boundary conditions on the first and the second eigenfrequency of a shell with and without internal heavy fluid loading is studied. A strong added mass effect is observed, especially for thin shells. Finally, it is shown that substantial suppression of the energy transmission in a semi-infinite cylindrical shell with and without internal heavy fluid loading is feasible in a relatively broad frequency range, both for vibration in the 'beam-type' mode $m = 1$ and in the mode $m = 2$. This effect of a frequency band gap is already achieved to some extent when a structure is composed of the minimum number of alternating elements (only one cell of periodicity). In all reported cases, predictions obtained by use of Floquet theory are found to be in a good agreement with an exact solution by the method of boundary integral equations.

Acknowledgement

The financial support provided to Dr. O.A. Ershova by the Centre for Machine Acoustics (Aalborg University) is gratefully acknowledged.

References

[1] C.R. Fuller, S.J. Elliott, P.A. Nelson, *Active Control of Vibration*, Academic Press, London, 1995.
[2] D.J. Mead, *Passive Vibration Control*, Wiley, New York, 1998.
[3] S.V. Sorokin, O.A. Ershova, Plane wave propagation and frequency band gaps in periodic plates and cylindrical shells with and without heavy fluid loading, *Journal of Sound and Vibration* 278 (3) (2004) 501–526.
[4] C. Kittel, *Introduction to Solid State Physics*, seventh ed., Wiley, New York, 1996.
[5] L. Brillouin, *Wave propagation in periodic structures*, second ed., Dover, New York, 1953.
[6] A.L. Gol'denveiser, V.B. Lidskij, P.E. Tovstik, *Free Vibrations of Thin Elastic Shells*, Nauka, Moscow, 1979 (in Russian).
[7] S.V. Sorokin, J.B. Nielsen, N. Olhoff, Green's matrix and the boundary integral equations method for analysis of vibrations and energy flows in cylindrical shells with and without internal fluid loading, *Journal of Sound and Vibration* 271 (3–5) (2004) 815–847.